ICAS PAPER No. 72 - 49

AERODYNAMIC INTERFERENCE BETWEEN AIRCRAFT COMPONENTS:
THE POSSIBILITY OF PREDICTION

by
Th. E. Labrujere, Senior Research Engineer and
H. A. Sytsma, Research Engineer
National Aerospace Laboratory (NLR)
Amsterdam, The Netherlands

The Eighth Congress of the International Council of the Aeronautical Sciences

INTERNATIONAAL CONGRESCENTRUM RAI-AMSTERDAM, THE NETHERLANDS
AUGUST 28 TO SEPTEMBER 2, 1972

Price: 3. Dfl.

AERODYNAMIC INTERFERENCE BETWEEN AIRCRAFT COMPONENTS: ILLUSTRATION OF THE POSSIBILITY FOR PREDICTION

by

Th. E. Labrujere and H. A. Sytsma

National Aerospace Laboratory NLR, Amsterdam

The Netherlands

Abstract

The availability of large capacity computers has widely increased the possibility of predicting aerodynamic interference between aircraft components. An example of the numerical methods developed recently for that purpose is the NLR-panelmethod. In the present paper the capability of this method is illustrated by means of application to complex configurations, such as wing-pylon-store combination and a wing-body-tail configuration. From comparison with experiments it appears that interference effects may be well predicted. In order to be able to represent correctly the effect of free vortexsheets in cases where this is required, this method has been extended with a procedure to determine the correct force-free location of the wake behind a wing. This procedure is illustrated by means of some preliminary results for a rectangular wing.
The effect of vortexsheet location has also been calculated for a conventional wing-body-tail configuration.

Contents

List of symbols

C	wing chord
C_p	pressure coefficient
C_p^*	critical pressure coefficient
C_M, C_m	pitching moment coefficients
C_L, C_ℓ	lift coefficients
Ma	Mach number
$\bar{n}$	unit normal
U_∞	onset flow velocity
V_m	mean velocity
x,y.z	cartesian co-ordinates
α	angle of attack
φ	perturbation potential
Γ	vortex strength
γ	vortex density

subscripts

b	refers to the body
t	refers to the trailing edge
w	refers to the wake
α	refers to th free-stream axis system

1. Introduction

The problem of aerodynamic interference between thick, lifting aircraft components is one of great interest in aircraft design. For instance the classical problem of wing induced downwash at the tail is still one of major importance. Also, the special requirements that have to be met in the design of modern high speed aircraft call for the possibility to predict in detail wing-body interference and the interference effects on wing-pylon-store or wing-nacelle arrangements.

An important contribution to the solution of such problems has been given by A.M.O. Smith and his colleagues (ref. 1) at the Mc Donnel-Douglas Corporation.
In their incompressible potential flow method the surface of an arbitrary non-lifting body is represented by plane quadrilaterals. A source density is applied to each surface element so as to satisfy the condition of zero normal velocity at each of the panel centroids. This leads to a system of linear simultaneous equations for the unknown source strengths. The solution of this system leads to the velocities and pressures in the control points (centroids).

The method was extended by Rubbert et. al. (ref. 3) of the Boeing Company who introduced lift by adding to the source distribution a horse-shoe vortex system inside the configuration with trailing vortices to represent the wake. At NLR

the applicability of the method was extended to high subsonic flow by the introduction of an appropriate set of semi-empirical compressibility corrections. Also, the computation times involved could be reduced drastically by applying a special iterative procedure to solve the large system of simultaneous equations.

The present paper is concerned with the application of the NLR-panel method to different types of interference problems such as the influence of a rear-mounted nacelle on wing characteristics and the problem of wing-pylon-store interference for a fighter-type wing with tiptank.

The last part of the paper deals with the problem of wing-body-tail interference. Because of the fact that for the calculation of the forces on a tailplane in the vicinity of a wake it is necessary to know the correct (force-free) position of the trailing vortices an iterative procedure has been developed to determine this position. The numerical features of this procedure will be discussed, together with a comparison between calculated and experimental results when applied to a rectangular wing at high incidence.

The method has been applied to a configuration with tailplanes. The pressure distributions as well as the overall characteristics have been determined and are compared with experimental data.

2. Outline of the method

2.1 Formulation of the problem.

Within the NLR panel method the inviscid compressible flow around an aircraft configuration is approximated by applying Göthert's rule in order to reduce the given problem to the solution of Laplace's equation. A consequence of this approach is, that locally the necessary simplifying assumptions concerning the magnitude of the perturbation velocity may be violated. Therefore allowance has been made for non-linear compressibility effects, by a set of semi-empirical compressibility rules.

Leaving aside the details of this approach which may be found in reference 7, the description of the method will be limited to the panel-method for the determination of the incompressible flow around an aircraft configuration. This problem is formulated schematically in figure 1.

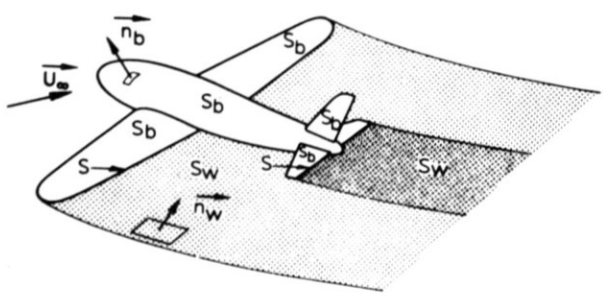

fig. 1 Illustration of the incompressible flow problem.

The flow is assumed to be irrotational everywhere outside the body and its wake so that Laplace's equation for the perturbation potential

$$\varphi_{xx} + \varphi_{yy} + \varphi_{zz} = 0 \qquad (1)$$

has to be solved for the boundary conditions

$$\varphi = 0 \qquad (2)$$

at infinity upstream, and

$$\frac{\partial \varphi}{\partial n} = -\bar{n}_b \cdot \bar{U}_\infty \qquad (3)$$

at the surface of the body, where n is the unit outward normal to the surface S_b and $\bar{U}_\infty$ is the onset flow velocity.

The wake behind the configuration is represented by a surface of discontinuity which extends downstream from a given line S on S_b where the wake has its origin. On wings and tailplanes this line coincides obviously with the trailing edge. The further downstream location of the surface of discontinuity then follows from the Kutta condition of smooth flow at the trailing edge and the requirement of zero pressure jump across this surface.

The requirement of zero pressure jump across the discontinuity surface implies that this surface should be a streamsurface so that

$$\frac{\partial \varphi}{\partial n} = -\bar{n}_w \cdot \bar{U}_\infty \qquad (4)$$

on S_w.

As the flow is assumed to be irrotational the surface of discontinuity is composed of curves along which the jump in velocity potential is constant and which coincide with streamlines. As such their position is uniquely determined, but since their position is unknown a priori the problem formulated above has a non-linear character.

It has been found that for many practical applications this non-linearity can be disposed of by estimating the position of the surface of discontinuity and by applying boundary condition (4) only at its origin S.

2.2 Solution of the boundary value problem.

Assuming the location of the surface of discontinuity the problem described above reduces to a boundary value problem of the Neumann type. This problem can be solved by expressing φ in terms of surface distributions of singularities (see e.g. Lamb, ref. 2). For practical purposes, discussed a.o. by Hess and Smith (ref. 1) and Rubbert et.al. (ref. 3) the following representation is suitable:

- source densities are distributed on the rigid surface S_b of the configuration
- a doublet representation with constant strength along the mean streamlines is chosen for the surface of discontinuity S_w.

Application of the boundary conditions mentioned above then leads to a system of integral equations for the unknown source and doublet strengths.

The solution to this system of integral equations is obtained numerically. For that purpose the surface S_b is, following Hess and Smith (ref. 1), represented by quadrilateral panels each carrying a constant source density (fig. 2). The

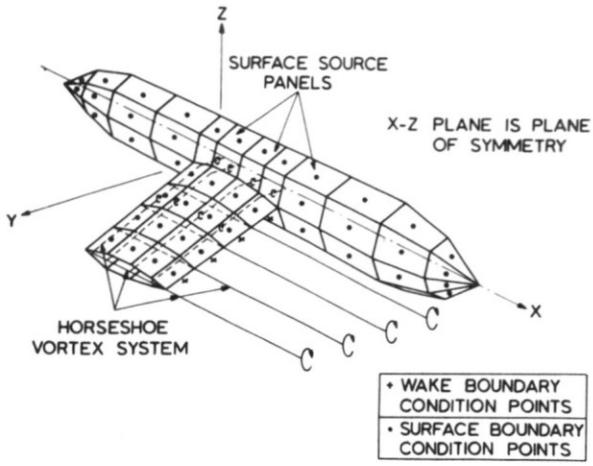

fig. 2 Schematic view of selected system of singularity distributions.

surface of discontinuity S_w is covered with streamwise strips each of which carries a constant doublet density. The doublet sheet is extended inside the configuration as in the method of Rubbert et.al. (ref. 3). Inside the configuration, the doublet strength in a strip is increased step by step from zero to the value in the wake. The magnitude of the steps is a prescribed empirical function of the doublet strength in the wake. The doublet sheet as described above is equivalent to a system of horse shoe vortices as sketched in fig. 2. The strength of the sources and the vortices is determined simultaneously in such a way that the boundary condition (3) is satisfied at the centroids of the surface source panels and that (4) is satisfied at a small distance from the origin of the wake in each doublet strip.

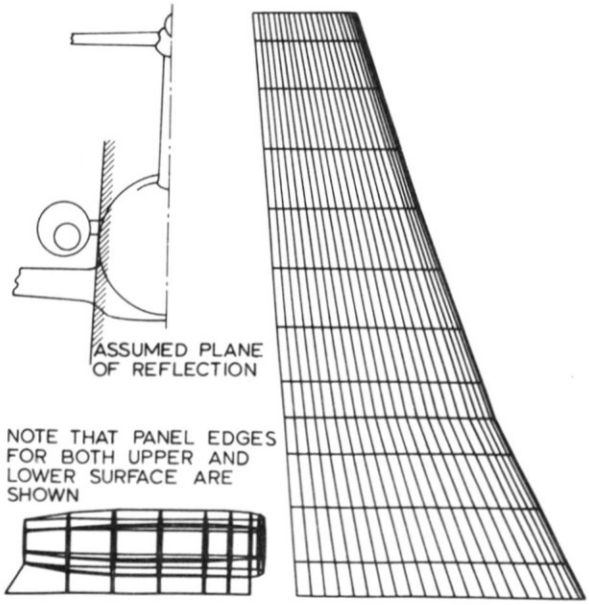

fig. 3 Panel arrangement and schematic rear view of wing-nacelle configuration.

The procedure sketched above leads to a system of linear equations for the unknown source and vortex strengths. This is solved by means of an iterative process described in ref. 5. At present up to 1800 equations can be dealt with on a CDC 6600 computer. The central processor time involved with such a system is about 35 minutes.

2.3 Some examples of application.

Since in an earlier paper (ref. 5) has been dealt with wing-body interference extensively, attention will be paid now to two other types of interference problems.

On account of the final remark in sect. 2.1, in both examples the wake has been assumed to be parallel to the longitudinal axis of the configurations considered.

In the first place the effect of a rear-mounted nacelle on the flow around a wing will be considered. A schematic rear view of the configuration, together with the panel-arrangement used are shown in fig. 3. Because of the fact that in this investigation stress was laid on the effect of the nacelle on the wing, rather than on predicting accurately the flow field around the complete configuration, use has been made of the well-known reflection-plane concept. The engine nacelle has been treated as a coarsely panelled ring-wing (annular free duct) and has been placed with its stub-wing against the reflection plane at the side of the fuselage.

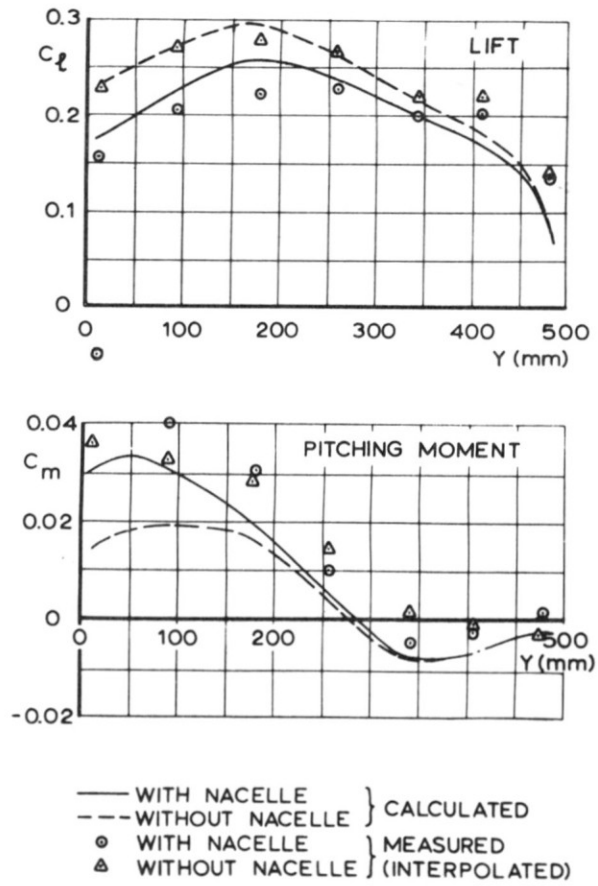

fig. 4 Comparison of measured and calculated section aerodynamic coefficients of wing-nacelle configuration.

A comparison of calculated and measured results for Ma = .64 and α = .43° is given in fig. 4 in terms of spanwise lift and pitching moment distributions. It can be noticed that the nacelle induces a significant reduction of C_ℓ and increases the pitching moment. From the comparison with experimental data it may be concluded that the main effect of the nacelle is well predicted.

A more complicated problem is the interference of wing, pylon and store of the configuration depicted in fig. 5. This problem has several aspects. In the first place the aerodynamic characteristics of the wing may change significantly by the presence of pylons and stores. This can lead to stability and control problems. Secondly there is the question of store separation characteristics. These are determined for a large part by the aerodynamic interference at the initial position, when the store is still attached to the pylon.

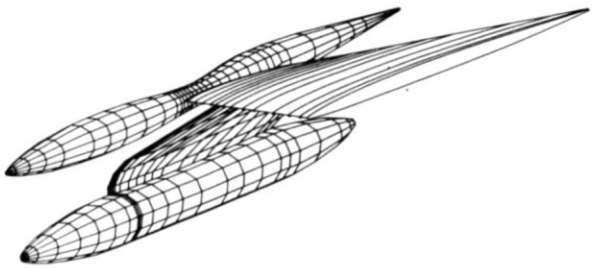

fig. 5 Panel arrangement of wing-tiptank-pylon-store configuration.

A comparison of measured and calculated spanwise lift distributions on the wing at Ma = .8 and α = 3° for the configuration with and without pylon/store is given in fig. 6. As usual the lift is overestimated as a result of the fact that viscous effects have not been taken into account.

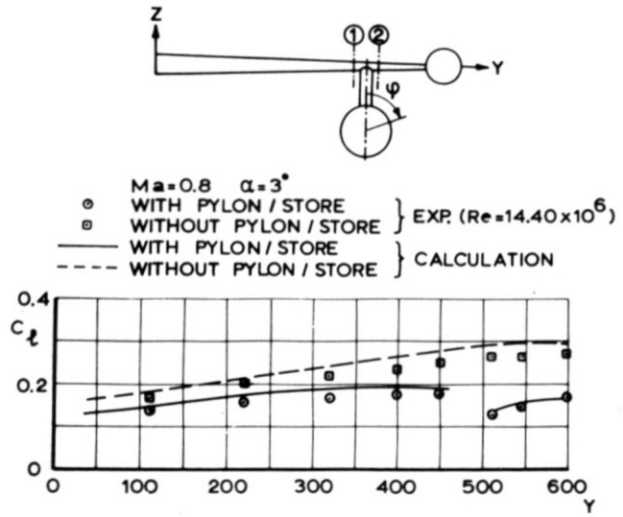

fig. 6. Spanwise liftdistribution on wing.

However the qualitative agreement is good and the effect of pylon and store is predicted reasonably well. Chordwise pressure distributions at two wing sections close to the pylon are presented in fig. 7. Again the qualitative agreement is good, although there is some discrepancy on the lower surface.

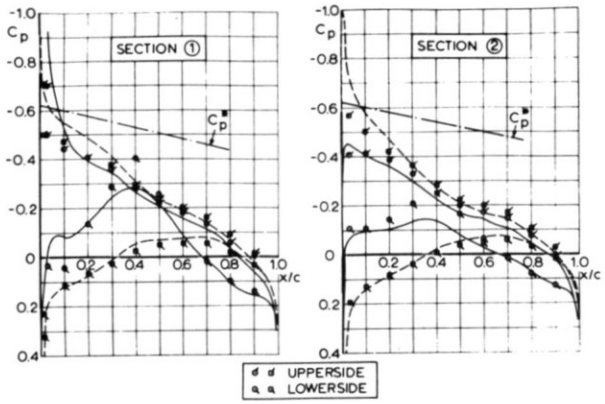

fig. 7 Chordwise pressure distributions on wing (Ma = .8, α = 3°).

It may be noted that the significant loss of total lift induced by the presence of the pylon and the store is due mainly to a rise of the mean velocity level on the lower side of the wing. Furthermore it should be remarked that the pressure in the nose region exceeds locally the critical pressure (fig. 7), so that, at least locally the predicted pressures are unreliable due to the fact that the present method essentially applies to onset flow Mach numbers below the critical value.

Store pressure distributions are given in fig. 8. They are predicted very well. In spite of the simple and arbitrary wake conception used for the store, i.e. with the trailing vortices of the store located in the plane of the wake behind the pylon.

3. Determination of overall-forces and moments of a wing-body-tail configuration.

3.1 General remarks.

It has been found from several applications and numerical experiments that the pressures on the wing and a large part of the fuselage are rather insensitive to differences in the wake representation behind the fuselage.

It may be expected however that in some cases both the location of the surface of discontinuity behind the wing and the representation of the wake behind the fuselage will have a definite influence on the pressure distribution over the rear part of the fuselage as well as on the tail planes. Then the overall forces and moments can only be determined with appreciable accuracy if the wake behind the wing and fuselage is represented correctly. It is assumed, that the main effect of the wake will be due to interference of the aircraft with the wake behind the wing.

Therefore an iterative procedure has been developed to determine the correct vortexsheet location behind a wing which will be described in the next section.

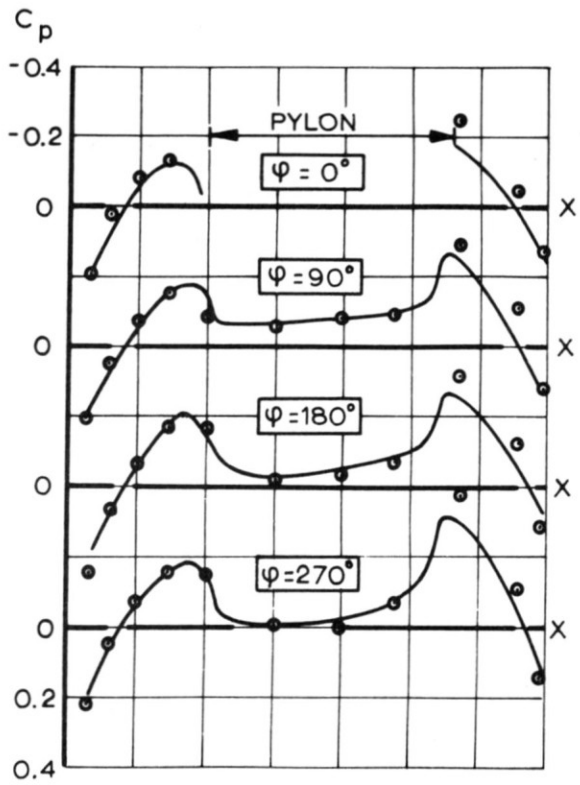

fig. 8 Store pressure distributions (Ma = .8, $\alpha = 3^{\circ}$).

3.2 Determination of the trailing vortexsheet location.

As has been remarked before, at given flow conditions the location of the trailing vortex-sheet behind a given configuration is uniquely determined when its origin on the body is given. This suggests that the location of the vortexsheet may be determined by means of an iterative procedure which starts with an estimate of the vortex sheet location. At NLR such a procedure has been developed by alternating the following two computations (see ref. 8):

1- determination of the strengths of sources and vortices for a given location of the vortex sheet
2- determination of the vortexsheet location for given strengths of sources and vortices.

The method developed at NLR for the determination of the vortexsheet location is in fact a simple extension of the panelmethod. It is based on relocation of the trailing vortices such that they fit into the streamline pattern.

Considering the flow around a wing in a plane normal to the trailing edge it may be observed that the vortex sheet should be located such that its tangent lies between the upper and lower wing surfaces. This is a consequence of the fact that the vortex sheet is a stream surface. For, if the sheet would be located such that its tangent lies above or below the wing, the flow would have to pass a convex corner. In general this would imply an infinite velocity and thus would violate Kutta's condition.

From this consideration it may be concluded, that there is always a corner concave to the flow, so that the component of the velocity normal to the trailing edge will be zero on upper or lower side of the sheet or on both sides.

From the further observation that the pressure jump across the vortexsheet should be zero, Mangler and Smith (ref. 4) derived some relations for the velocity components at the wing trailing edge, from which the behaviour of the vortexsheet at its origin may be determined.

The far-field influence of the discrete vortex system will be correct if its average vorticity density is the same as that of the continuous sheet. Considering the vorticity as a function of the arclength s measured along curves on S_w normal to the trailing vortices, this condition implies

$$\Gamma_i = \int_{s_i}^{s_{i+1}} \gamma(s)\, ds \qquad (5)$$

where Γ_i is the strength of a discrete vortex.

As far as the mean velocity is concerned, a vortex system satisfying this condition will have the correct near-field influence, within quadratic approximation of $\gamma(s)$, at points midway between two adjacent vortices.

It is assumed that, conversely, a correct distribution of discrete vortex strength is obtained by means of the panel method where the condition of tangential flow is imposed at the wake boundary points that are located midway between the vortices.

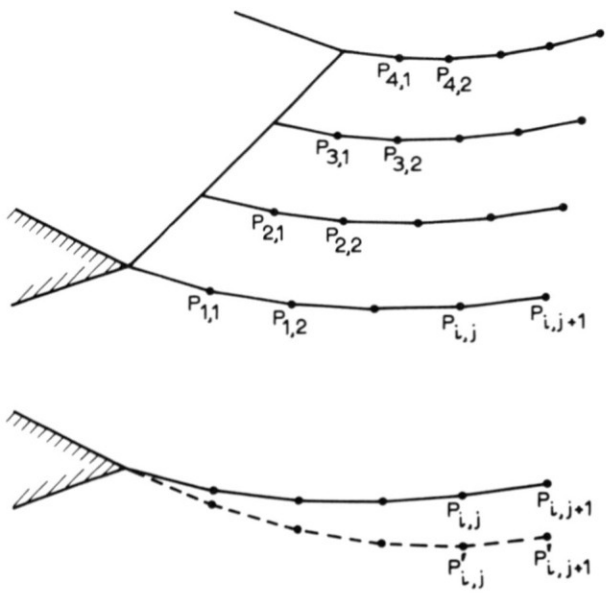

fig. 9 General arrangement of trailing vortex system.

Since the trailing vortices should coincide with streamlines the location of a point on a vortex is determined by

$$y_o = \int_{x_t}^{x_o} \frac{v_{m_y}}{v_{m_x}} dx + y_t \qquad (6a)$$

$$z_o = \int_{x_t}^{x_o} \frac{v_{m_z}}{v_{m_x}} dx + z_t \qquad (6b)$$

where the line integrals are taken along the vortex considered. By representing the vortices by a chain of straight-line segments and by taking the velocity ratio constant along those elements the integrals are evaluated by stepwise integration.

As the near-field influence of the vortices is only correct in points midway between the vortices, the velocity ratio at a point on a vortex will have to be determined by interpolation. Furthermore, it will be clear, that the correct streamline pattern on the vortex sheet cannot be determined directly from an assumed location of the trailing vortices, because of the non-linear character of eqs (6).

Therefore the following iterative procedure is applied. Let a first estimate of the vortex sheet location be given by a set of points $P_{i,j}$ (see fig. 9). The second estimate of the location of these points may then be obtained by evaluating the line integrals of eq (6) step by step. Suppose that the computation has advanced until the point $P'_{i,j}$ being the second estimate of $P_{i,j}$. Then the position of the point $P'_{i,j+1}$ is determined by

$$y'_{j+1} = \left[\frac{v_{m_y}}{v_{m_x}}\right]_{P_{i,j}} (x_{j+1} - x_j) + y'_j$$

$$z'_{j+1} = \left[\frac{v_{m_z}}{v_{m_x}}\right]_{P_{i,j}} (x_{j+1} - x_j) + z'_j \qquad (7)$$

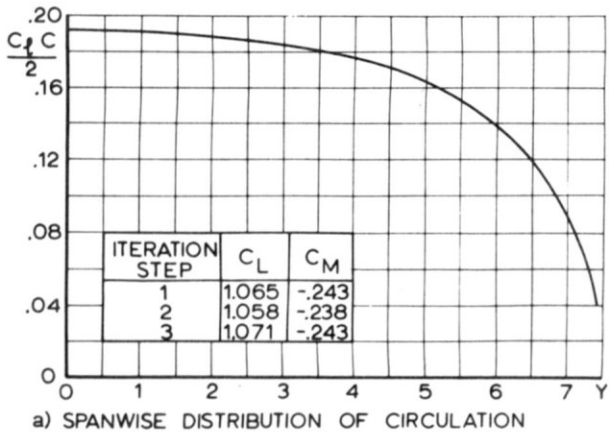

a) SPANWISE DISTRIBUTION OF CIRCULATION

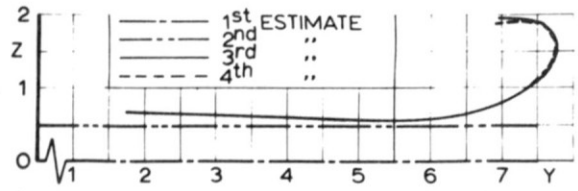

b) THE SHAPE OF THE VORTEX SHEET AT THE DOWNSTREAM STATION $\frac{X_\alpha - X_{\alpha_t}}{C} = 2$ ACCORDING TO FOUR SUCCESSIVE ESTIMATES

fig. 10

It is assumed that the velocity induced at $P_{i,j}$ by the singularity distribution on the body and the vortexsheet in its first estimated position may be assigned within first order approximation to the point $P'_{i,j}$.

Iterating this computation scheme until the discrepancies between two successive estimates are sufficiently small, the ultimate result may be considered as the correct position of the vortex sheet for the given strengths of sources and vortices.

In order to determine the vortex sheet location for given onset flow conditions the source and vortex strength will have to be determined again with the vortexsheet in its new estimated position. The whole process outlined above is iterated until sufficiently small discrepancies are obtained.

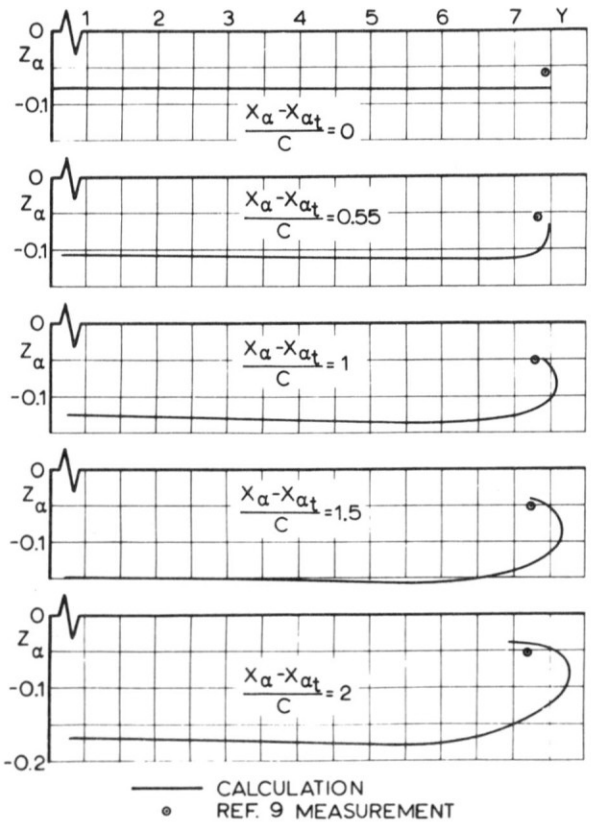

fig. 11 Comparison of calculated tip-vortex location with experiment.

The procedure for the determination of the trailing vortexsheet location may be illustrated with some results obtained for a rectangular wing of aspectratio 5 at an angle of attack of 15°.

The iteration process proceeded as follows. In the first step the strength of sources and vortices was determined with the vortexsheet located in the plane tangential to the camber surface of the wing. The spanwise distribution of the circulation thus found is depicted in fig. 10a.

From the velocity distribution along the trailing edge it was deduced that the vortexsheet should be tangential to the lower wing surface in order to fulfill Mangler's relations. Therefore in the second step the vortexsheet was assumed to be located in the plane tangent to the lower wing surface. For the source and vortex strengths thus found the vortexsheet location was determined in the third step. Recalculation of the strength of sources and vortices led to a fourth estimate of the vortexsheet location in the last step.
The shape of the vortexsheet in a plane x = constant at two chordlengths aft of the trailing edge is depicted in fig. 10b. It may be seen that the successive estimates show a definite convergence of the iteration process. A comparison with limited experimental results is presented in fig. 11. At a few downstream sections the shape of the calculated vortexsheet is depicted. The circular symbol indicates the location of the tipvortex as found in experiments performed at NLR. It may be noted that the agreement is satisfactory. A three-dimensional side view of the calculated vortexsheet is presented in fig. 12.

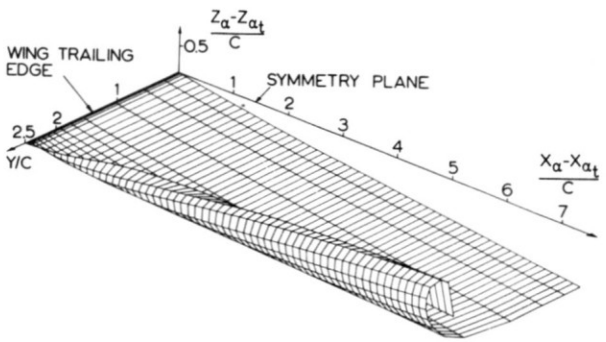

fig. 12 Side view of trailing vortexsheet of rectangular wing of aspectratio 5 (α = 15°, C_L = 1.0).

The spanwise distribution of circulation determined during this calculations appeared to coincide within drawing accuracy. The variation of the overall lift and moment coefficients was very small. Moreover, the values determined at the fourth step of the iteration process, with the vortexsheet close to its correct position, appeared to be almost identical to those determined in the first step.

These results demonstrate the fact that the flow around the wing is rather insensitive to the location of the trailing vortexsheet and thus seem to justify the assumption of the vortexsheet to be tangential to the wing camber surface, which is common practice when the flow around a wing is determined.

3.3 Discussion of the results for a wing-body-tail configuration.

The configuration considered is a typical short-range subsonic aircraft, schematically depicted in fig. 13.

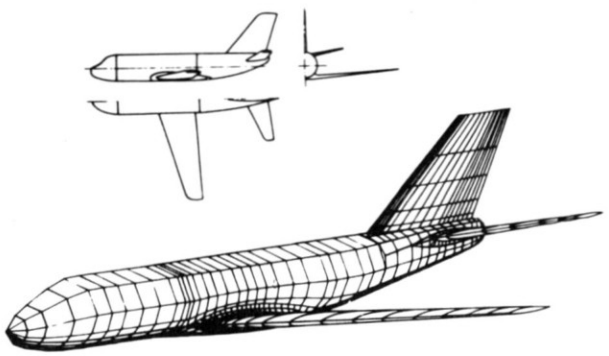

fig. 13 General arrangement and panel plot of wing-body-tail configuration.

The conditions for which the calculations have been performed are: Machnumber of onset flow Ma = .4 and angles of attack α = .2° and 6.37°. Fig. 13 gives also an impression of the distribution of panels used at these calculations.

As far as the representation of the wake is concerned the following remarks may be made.
With respect to the fuselage it should be noted that the representation of its wake by a surface of discontinuity emanating from a given line is highly arbitrary.
Bearing in mind also that an isolated fuselage in uniform flow carries relatively little lift, it is usually assumed at NLR that the fuselage sheds no vorticity at all.
As it has appeared that differences in the location of the vortexsheet behind a wing have little influence on the pressure distribution over the wing itself, it seems justified to assume that the vortexsheet behind the tailplane may be given a fixed estimated location.

A first calculation was performed with the wake of the wing parallel to the longitudinal axis of the configuration. It may be expected that for the present configuration, at least at moderate angles of attack, the stabilizer is relatively remote from the actual location of the wake of the wing, and that therefore the displacement of the wake will have only little influence. Yet, to be sure, the force-free position of the surface of discontinuity was calculated according to the procedure outlined above.
The magnitude of the displacement with respect to the first estimate of the wake position may be illustrated with the aid of fig. 14, where a cross section of the wake in the neighbourhood of the stabilizer is depicted. It may be seen that the displacement is hardly visible for α = .2° and still very small for α = 6.37°.

Recalculation of the pressure distribution on the aircraft with this improved estimate of the location of the wake behind the wing, led to the results presented in fig. 15. Here a comparison

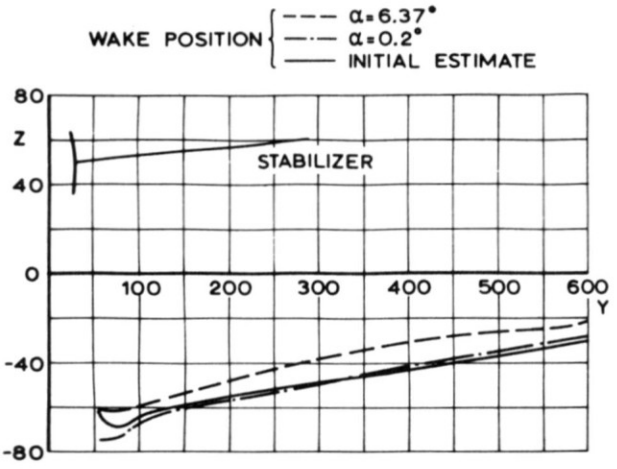

fig. 14 Wake positions at horizontal stabilizer.

is made between the calculated pitching moment versus lift curve for the first estimated position of the wake indicated by the dash-dot lines, the second estimated position of the wake indicated by the solid lines and the experimental results.

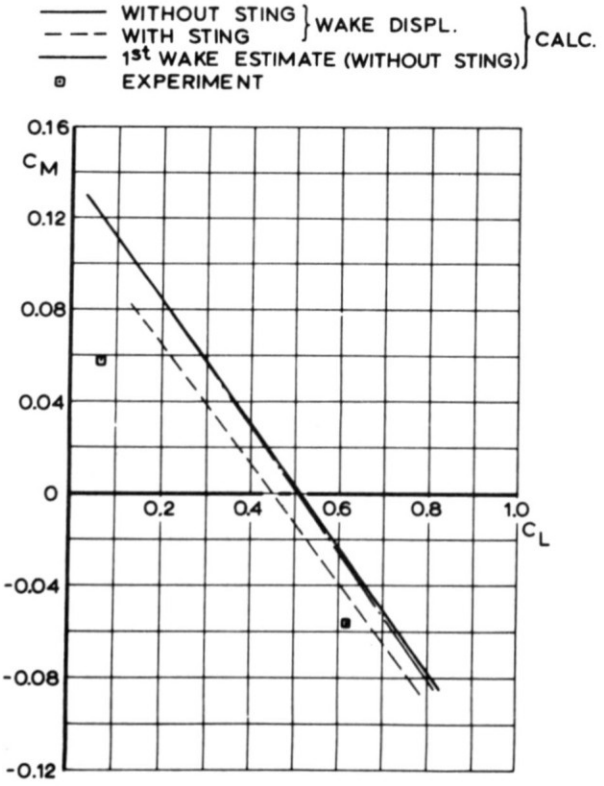

fig. 15 Total pitching moment versus total lift.

It may be seen that the influence of the wake displacement is indeed hardly visible. Furthermore the agreement with the experimental results is not quite satisfactory. Although the general tendency of the pitching moment-lift relation is predicted reasonably, the calculated curve is shifted with respect to the measured one and there is also a difference in slope. It seems, that these discrepancies are too large for attribution to viscous effects only.

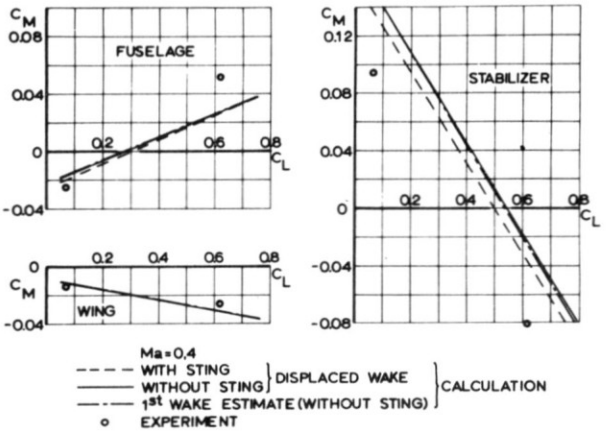

fig. 16 Contribution to the pitching moment of parts of the configuration.

By considering the separate contributions of wing, fuselage and stabilizer to the total pitching moment, as depicted in fig. 16, it is found that the stabilizer and the fuselage are mainly responsible for the discrepancies.
The slope of the pitching moment-lift curve on the stabilizer seems to be predicted rather well, but there is a constant shift. With respect to the fuselage it may be remarked that for $\alpha = .2^{\circ}$ the agreement is fair while for $\alpha = 6.37^{\circ}$ the discrepancy is significant. From fig. 18 it follows further that the effect of the wake displacement on the lift of the stabilizer is not visible for $\alpha = .2^{\circ}$, while for $\alpha = 6.37^{\circ}$ it is hardly noticeable.

From these results it may be concluded that the calculations thus performed do not suffice to predict the aerodynamic characteristics of the windtunnelmodel completely satisfactorily. It seems that apart from boundary layer influence, there are rather important effects that have not been taken into account.
To the opinion of the authors the main effects that may be hold responsible for the discrepancies are interference with the model sting support, tunnelwalls and neglection of vortexshedding from the fuselage.

In order to investigate the interference effect of the sting the pressure distribution on the configuration has been recalculated with the vortexsheet behind the wing in its second estimated position. The relevant results are indicated in fig. 15 by the dashed line. It may be seen that indeed a significant improvement of the numerical results is obtained. From fig. 16 it appears that the main effect of the sting is concentrated at the stabilizer, while from fig. 17

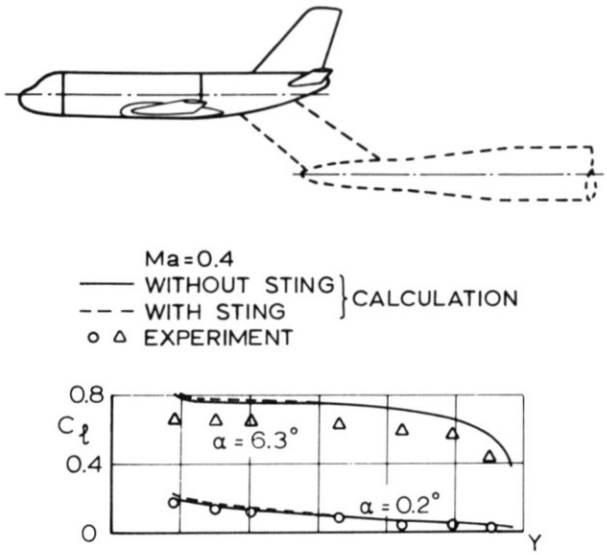

fig. 17 Spanwise liftdistribution on wing.

it may be seen that the liftdistribution on the wing is hardly influenced. The liftdistribution on the stabilizer is improved as may be seen from fig. 18, but there still remains a discrepancy which is independent of the angle of attack.

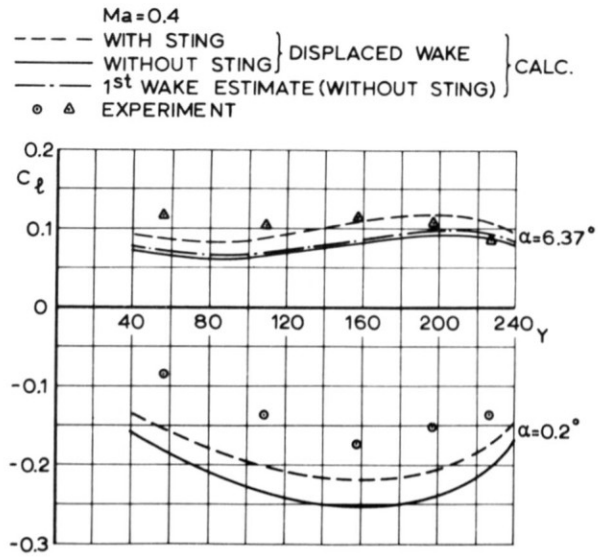

fig. 18 Spanwise liftdistribution on stabilizer.

With respect to the other sources for discrepancy the following remarks may be made. In the first place the neglection of vortex shedding from the fuselage might have been to crude an approximation. Possibly, the introduction of vortex shedding could improve the agreement with measurement, however in that case one would expect the influence on the stabilizer to depend on α.

Secondly tunnelwall influence has not been taken into account. Generally this influence can be treated as a linear combination of lift-interference effects and blockage effects. According to ref. 10 blockage effects in the NLR-High-Speed-Tunnel are negligible, while lift-interference, if significant would also be a function of C_L.

Thus the remaining discrepancy for fuselage and stabilizer cannot be explained with the material collected so far, and further investigation is needed.

Acknowledgement

The authors are indebted to mr. J.W.Slooff for his valuable advice and criticism. Also thanks are expressed to messrs. F.J.Heerema, Th.Janssen and G.H.Nijhuis for their assistance in preparing and carrying-out the actual calculations.

4. References

1 Hess, J.L. and Smith, A.M.O. — Calculation of potential flow about arbitrary three-dimensional bodies. Douglas Aircraft Corp.Rep. ES 40622 (1962)

2 Lamb, H. — Hydrodynamics. Cambridge Univ.Press. London (1932)

3 Rubbert, P.E. et.al. — General method for determining the aerodynamic characteristic of fan-in-wing configurations. USAAVLABS Techn.Rep. 67-61A

4 Mangler, K.W. and Smith, J.H.B. — Behaviour of the vortexsheet at the trailingedge of a lifting wing. RAE TR 69049 (1969)

5 Labrujere, Th.E. Loeve, W. and Slooff, J.W. — An approximate method for the calculation of the pressure distribution on wing-body combinations at subcritical speeds. AGARD AP. no. 71 paper 11 (1970)

6 Loeve, W. and Slooff, J.W. — On the use of panel methods for predicting subsonic flow about aerofoils and aircraft-configurations. 4 Jahrestagung of DGLR, Baden-Baden (1971) NLR MP 71018

7 Loeve, W. and Slooff, J.W. — A method for the calculation of pressure distributions on wing-body combinations in subcritical attached flow. NLR report to be published.

8 Labrujere, Th.E. — A numerical method for the determination of the vortex-sheet location behind a wing in incompressible flow. NLR report in preparation.

9 de Vries, O. Experimental investigation of the vortex wake behind a swept back wing.
NLR TR 72017.
Report in preparation.

10 Loeve, W. On the subsonic wall-interference effects in the high speed tunnel HST of NLR.
NLR TM T.167.